



|                        |  |
|------------------------|--|
| Title                  | Ultra-high Water Content Photonic Hydrogels with Large Electro-Optic Responses in Visible to Near-Infrared Region  |
| Author(s)              | Youfeng, Yue; Yasuo, Norikane; Jian Ping, Gong   |
| Citation               | Advanced Optical Materials, 9(9), 2002198<br><a href="https://doi.org/10.1002/adom.202002198">https://doi.org/10.1002/adom.202002198</a>   |
| Issue Date             | 2021-05-05   |
| Doc URL                | <a href="http://hdl.handle.net/2115/85098">http://hdl.handle.net/2115/85098</a>  |
| Rights                 | This is the peer reviewed version of the following article: Ultra-high Water Content Photonic Hydrogels with Large Electro-Optic Responses in Visible to Near-Infrared Region, which has been published in final form at <a href="https://onlinelibrary.wiley.com/doi/10.1002/adom.202002198">https://onlinelibrary.wiley.com/doi/10.1002/adom.202002198</a> . This article may be used for non-commercial purposes in accordance with Wiley Terms and Conditions for Use of Self-Archived Versions. |
| Type                   | article (author version)   |
| Additional Information | There are other files related to this item in HUSCAP. Check the above URL.   |
| File Information       | 20210201-manuscript.pdf  |



[Instructions for use](#)

# **Ultrahigh-water-content photonic hydrogels with large electro-optic responses in visible to near-infrared region**

Youfeng Yue<sup>a,b,c,\*</sup>, Yasuo Norikane<sup>a</sup>, Jian Ping Gong<sup>d</sup>

<sup>a</sup>Research Institute for Advanced Electronics and Photonics, National Institute of Advanced Industrial Science and Technology (AIST), Tsukuba, 305-8565, Japan.

<sup>b</sup>PRESTO, Japan Science and Technology Agency, Kawaguchi 332-0012, Japan.

<sup>c</sup>Graduate School of Life Science, Hokkaido University, Sapporo 001-0021, Japan.

<sup>d</sup>Faculty of Advanced Life Science, Institute for Chemical Reaction Design and Discovery, Soft Matter GI-CoRE, Hokkaido University, Sapporo, Hokkaido, 001-0021, Japan.

E-mail: yue-yf@aist.go.jp

## **Abstract**

The embedding of photonic crystals within stimuli-responsive hydrogels has attracted tremendous interest because it provides new applications such as optical switches, displays, and sensors, among others. However, the production of electrically tunable photonic hydrogels with a wide range of color tunability, fast electrical response, and high stability for repeated use is still a challenging task. Here, electrically tunable photonic hydrogels were fabricated using ultrahigh-water-content polyelectrolyte layered hydrogels composed of thousands of bilayer domain structures. The layered hydrogel developed in this work exhibited versatile color tunability by applying an electric field

parallel or perpendicular to the direction of the gel layers. The hydrogel exhibited homogeneous color tuning when a perpendicular electric field was applied, while it showed a large rainbow-like electric-optic response in the visible to near-infrared region when a parallel electric field was applied. Additionally, by a simple method using patterned electrodes, a reflective display showing the designed characters was demonstrated and maintained for hours under water without an external source of energy. Moreover, the electrically induced optical pattern can be erased, and the responsive photonic hydrogel showed excellent stability for repeated use. We anticipate that this study will provide the foundation for the development of responsive photonic hydrogels with new and large electro-optical effects for future chromatic applications.

## **1. Introduction**

Natural structural colors, such as those exhibited by *Morpho* butterflies, beetles, and tropical fish, have attracted considerable attention in various research fields and inspired several optical devices.<sup>[1]</sup> The bright colors exhibited by nature result from the interaction of light with periodic nanostructures by interference, scattering, or diffraction.<sup>[2]</sup> Artificial photonic crystals that mimic these natural nanostructures, or their optimal functions, have found practical applications in optoelectronic devices, including optical filters, transistors, light-emitting diodes, lasers, and chemical and biological sensors.<sup>[3-10]</sup> Since photonic crystals can inherently display structural colors without using light-emitting elements, only by reflecting specific bands of wavelength from the environment, the development

of photonic crystals for paper-like full-color displays is an intense area of research. Among photonic crystals, soft photonic crystals have attracted significant attention not only because of their un-faded bright color but also because of their stimuli-responsive nature.<sup>[4][11]</sup> Soft photonic crystals can be integrated into scalable flexible substrates and tuned to any color in response to external stimuli. Additionally, the color displayed by soft photonic crystals is visible under ambient conditions, either in a bright room or outdoors under sunlight, which meets the fundamental requirement for practical mobile display applications. Despite the apparent technological and scientific progress in soft photonic crystals as backlight-free displays, reports on electrically tunable photonic crystals are still scarce.<sup>[12-22]</sup> Probably, because developing highly electrically responsive photonic crystals, whose refractive index contrast and/or lattice dimension can be continuously, reversibly, and rapidly tuned by electrical or magnetic stimuli, is a difficult task. The research to date reports photonic crystals showing only one trend of color change, either a blue-shift or red-shift upon voltage change. Arbitrary and reversible color patterning on photonic crystals using electric/magnetic stimuli is still challenging. The earliest sample of electrically tunable photonic crystals was designed based on an electroactive metallopolymer/silica opal composite.<sup>[13]</sup> Due to the loss of electrons from the metallopolymer under an electric field, the surrounding electrolyte ions enter the photonic crystals to neutralize the positive charge, which increases the spacing between the silica beads and induces a red-shift in color.<sup>[13]</sup> In addition to the electron-ion migration mechanism, polyelectrolyte hydrogels are well known for their volume change

in response to an electric field.<sup>[23-24]</sup> Additionally, the volume change of hydrogels can be controlled by hydrated ion migration, which is affected by the charge density in and out of the hydrogels. Previously, layered photonic hydrogels with color tunability driven by mechanical stimuli have been synthesized, which contained thousands of nanometer-scale polymerized dodecylglyceryl itaconate (PDGI) bilayers and soft gel layers.<sup>[25-28]</sup> However, large and tunable electric-optic response in layered photonic hydrogels has not been demonstrated.

Here, electrically tunable photonic hydrogels were fabricated using ultrahigh-water-content polyelectrolyte layered hydrogels composed of thousands of bilayer domain structures. Dynamic color tuning in 1D photonic hydrogels by applying an electric field perpendicular or parallel to the direction of the hydrogel layers has been demonstrated for the first time. The photonic hydrogel exhibited uniform color tuning when a perpendicular electric field was applied, while it showed a unique rainbow-like color from blue to near-infrared when applying a parallel electric field to the layers. Additionally, by a simple method using patterned electrodes, a reflective display showing the printed characters was demonstrated. We anticipate that these electric-optic responsive soft materials will find interesting application in displays, sensors, or other electrochromatic systems.

## **2. Results and Discussion**

### **2.1 Design of electrically tunable photonic hydrogels**

The fabricated high electroactive photonic hydrogels are shown in **Figure 1**. The initially

synthesized parent photonic hydrogels (water content ~90wt%) did not show any electrical response due to the absence of polyelectrolytes in the polymer network.<sup>[26]</sup> To make it electrically responsive, the photonic hydrogels were chemically treated with a sodium hydroxide (NaOH) aqueous solution (see experimental for detail). After the NaOH treatment, the hydrogel partially changed the polymer networks from polyacrylamide to sodium polyacrylate (PAAcNa) and swelled largely in water due to the high osmotic pressure of the dissociated counterions (**Movie 1**).<sup>[28]</sup> At the same time, the unidirectional PDGI bilayers in the parent photonic hydrogel were broken into small domains due to swelling along the bilayer direction. The so-prepared hydrogels reflect light in red or far-red wavelengths due to the increase in the water content (~98wt%) as well as the layer distance, up to ~ 300 nm (calculated from Bragg diffraction). These ultrahigh-water-content hydrogels thus introduced electro-responsive polyelectrolytes into the polymer network (**Figure 1a**). The nanometer-scale PDGI bilayer structures of the gel before and after the NaOH treatment were characterized by small-angle X-ray scattering (SAXS). The X-ray was imposed parallel to the bilayer plane. A broad peak clearly appeared at  $2\theta=2^\circ$ , corresponding to a thickness of ~ 4.4 nm, indicating that both the samples before and after the NaOH treatment retained the bilayer structure (**Figure S1**, Supporting Information). To study the orientation of the bilayer structure before and after the NaOH treatment, the 2D SAXS patterns and the azimuthal intensity distribution were obtained and are shown in **Figure 1b-c** and **Figure S2**, respectively. Before the NaOH treatment, an anisotropic scattering pattern, with an equatorial streak, was

observed (**Figure 1b**). After the NaOH treatment, the eccentricity of the elliptical shape in the 2D SAXS patterns almost disappeared (**Figure 1c**), indicating a structural change of the layer orientation in the gel matrix. This effect was also clearly identified by the broadened peaks of the azimuthal intensity after swelling (**Figure S2**). This structural change was attributed to the fracture of ordered bilayer membranes into bilayer domains after swelling.

To evaluate the mechanical properties of the hydrogels before and after the NaOH treatment, elongation/relaxation cyclic test in the direction parallel to the layer direction were carried out and are shown in **Figure 1d**. Before the NaOH treatment, the hydrogel exhibited a clear yielding, high Young's modulus of 0.196MPa, and large hysteresis area ( $16.3 \text{ kJ m}^{-3}$ ) due to the energy dissipated during dissociation of the bilayers upon deformation.<sup>[29-30]</sup> On the contrary, after treatment, the hydrogel showed no obvious yielding, a much smaller Young's modulus of 0.023MPa, and the hysteresis area was significantly decreased ( $2.3 \text{ kJ m}^{-3}$ ), indicating that the material with bilayer domains becomes soft and elastic. Thus, further modulation in the bilayer domain structure consumes little energy. Such structural and mechanical property changes enable the layered hydrogel to achieve a fast and large response to external electrical stimuli.

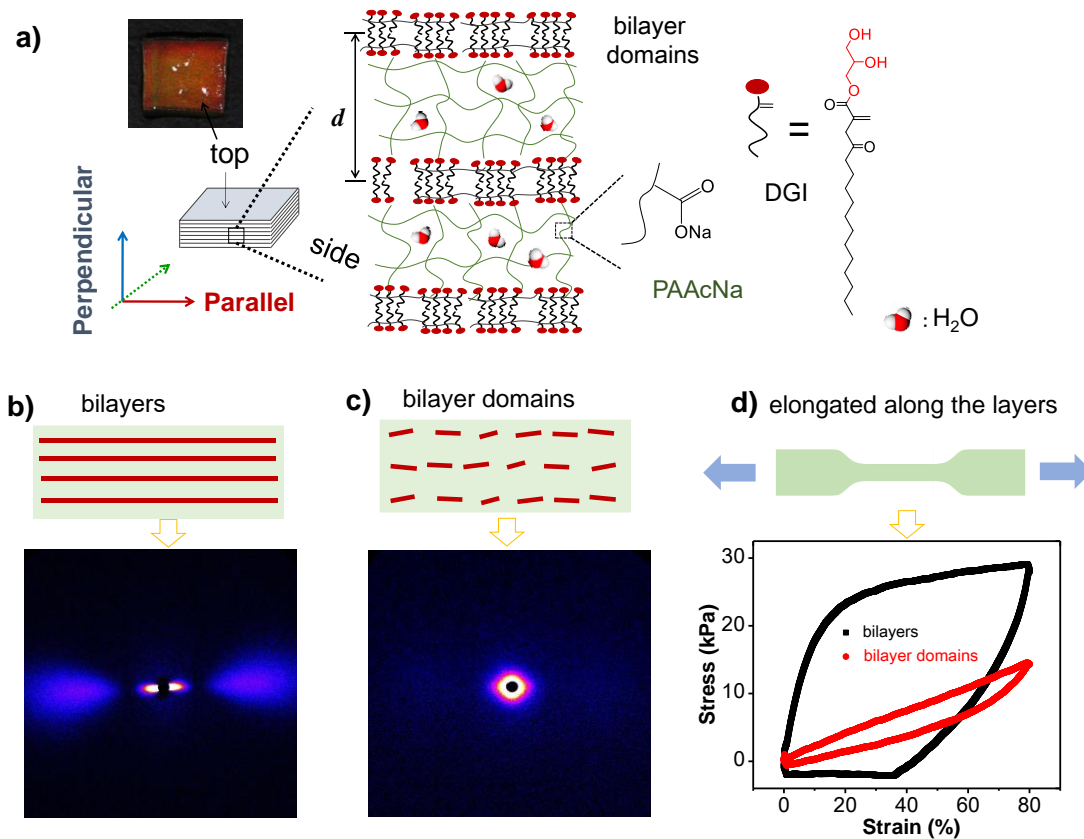


**Figure 1** a) Illustration of the structure of an ultrahigh-water-content polyelectrolyte photonic hydrogel with bilayer domain structure and inter-bilayer distance ( $d$ ). **b, c)** Schematics and 2D SAXS patterns of the parent hydrogel with bilayers and the NaOH treated hydrogel with bilayer domain structure. **d)** Their corresponding elongation/unloading stress–strain curves of the hydrogel with bilayer and bilayer domain structure, respectively.

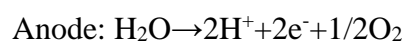
## 2.2 Effect of perpendicular electric field

We designed and demonstrated the dynamic color tuning in 1D polyelectrolyte hydrogels by controlling the direction of the electric field relative to the layered structure: perpendicular or parallel to the layers. **Figure 2** shows the schematic diagram of the



electrochemical cells and schematic representations of the mechanism for electrochemical color tuning of the photonic hydrogel. When an electric field perpendicular to the layers is applied to the cell, the layered hydrogel is expected to change color from red to green (or blue) by decreasing the inter-bilayer spacing  $d$  (**Figure 2a-b**). The polyelectrolyte layer of PAAcNa is an acidic polymer with ionized carboxylic groups as macroions and  $\text{Na}^+$  as counterions (**Figure 2b**). The carboxylate anions ( $-\text{COO}^-$ ) are fixed to the polymer network and are not mobile, while the  $\text{Na}^+$  cations, are mobile and easily exchange with other cations, especially with  $\text{H}^+$  ions, because the  $-\text{COO}^-$  has an order of cation selectivity  $\text{H}^+ > \text{Ca}^{2+} > \text{Mg}^{2+} > \text{K}^+ > \text{NH}_4^+ > \text{Na}^+ > \text{Li}^+$ .<sup>[31]</sup>

When an electric field is applied, electrolysis of water occurs at voltages above the electrolysis voltage of water ( $\sim 1.7\text{V}$ ). The electrochemical reactions on the two electrodes are as follows<sup>[24]</sup>:



Thus, there are  $\text{H}^+$  ions produced by electrolysis of the surrounding water in the vicinity of the anode. Then, the  $\text{H}^+$  ions diffuse into the hydrogel and exchange with  $\text{Na}^+$  ions to form carboxylic acid ( $-\text{COOH}$ ) in the polymer network. This ions exchange affects the swelling degree of the gel because the dissociation degree of  $-\text{COOH}$  group is much smaller than that of  $-\text{COONa}$  group (**Figure 2b-c**). As a result, the ionic osmotic pressure

decreases, and the polyelectrolyte gel layers shrink to show a blue shift of structural color.

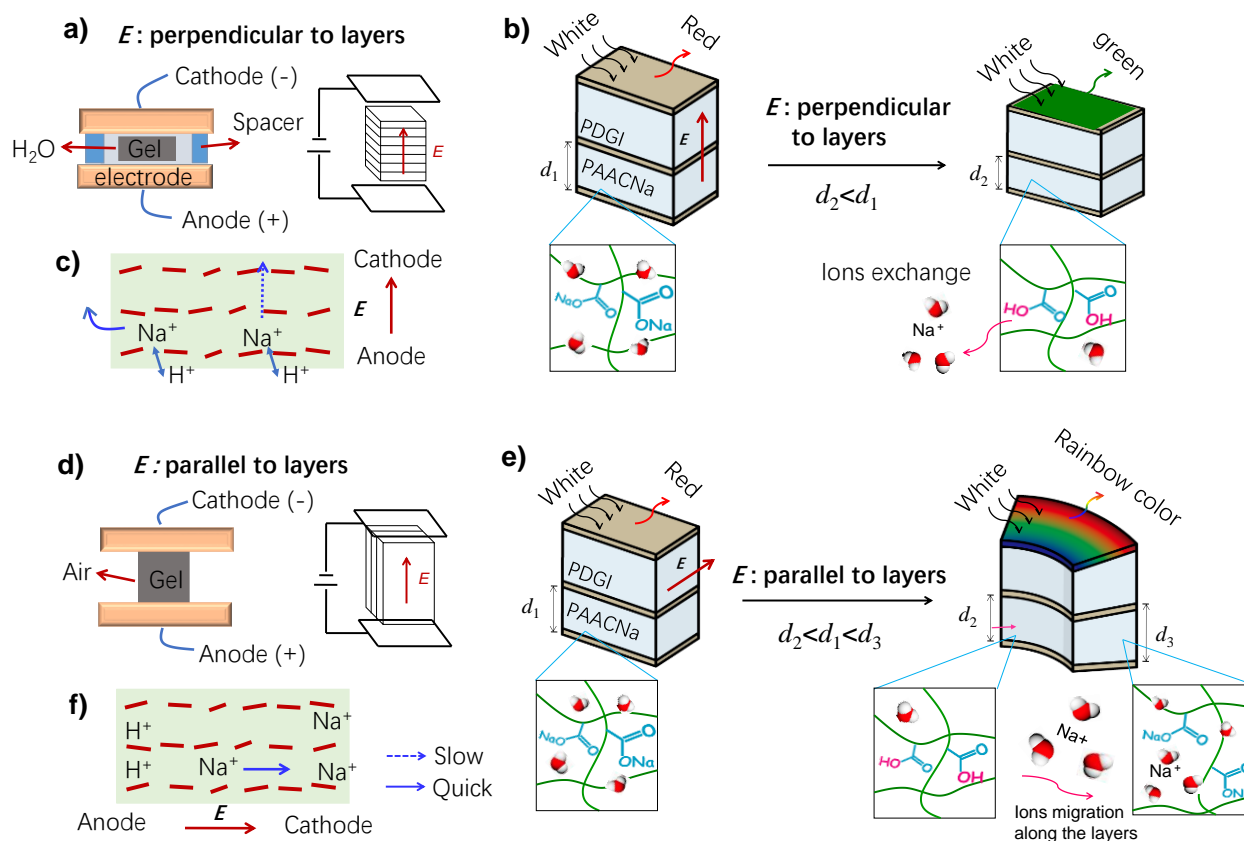


**Figure 2 Schematic diagram of electrochemical cells and schematic representation**

**of the mechanisms for their electro-optic response. a)** An electric field ( $E$ ) applied in the direction perpendicular to the gel layers. The thickness of the prepared polyelectrolyte hydrogel is 1.5-1.8 mm. The spacer is about 3 mm. The hydrogel was surrounded by water, not directly in contact to the two electrodes. **b)** The corresponding color tuning mechanism with perpendicular electric field. **c)** The ions exchange and migration in the layered hydrogel upon a perpendicular electric field. **d)** An electric field applied in the direction parallel to the gel layers. The hydrogel was directly in contact to the two electrodes (with no water surrounding). **e)** The corresponding color tuning mechanism

with parallel electric field. **f)** The ions exchange and migration in the layered hydrogel upon a parallel electric field.

Based on this assumption, we applied a voltage 8.0 V on a red-colored hydrogel in the direction perpendicular to the layers. As shown in **Figure 3a**, the color shifts from red to green with time. The reflection spectrum shows a blue shift from ~610–460 nm within 5 min. **Figure 3b** illustrates that the hydrogel displays time-dependent continuous shifts in the reflection spectra ~150 nm within 5 min. Upon the electric field, the H<sup>+</sup> ions (or pH value) in the surrounding water near anode follows a gradient concentration change along a direction perpendicular to the anode from the electrode surface; <sup>[12]</sup> the hydrogel thus exhibits an anisotropic swelling, *i.e.*, the surface close to the anode shrinks quickly and another side does not significantly change, resulting in the decrease in the peak intensity and a broadening of the reflection spectrum (**Figure 3a, Figure S3**). After the H<sup>+</sup> ions sufficiently exchange with Na<sup>+</sup> ions, the swelling degree of the gel gradually reaches the equilibrium collapsed state from anode to the other side. Then, the peak intensity of the new reflection spectrum increases (**Figure 3a, Figure S3**).

The blue shift of the color and the corresponding shift of the maximum wavelength ( $\lambda_{\max}$ ) under the electric field resulted from the decrease in the inter bilayer distance. The magnitude of the blue-shift in the total  $\lambda_{\max}$  increases with the increase of the voltages applied on the hydrogels (**Figure S4**). Increasing the applied voltage improves the

response speed of the hydrogel (**Figure S5**). The blue-shifted structural color is reversible. When the water in the cell was changed to an electrolyte solution (e.g., NaCl 0.4M), the color of the gel showed red-shift rather than blue-shift under the perpendicular electric field (**Figure S6**). This can be attributed to the higher Na<sup>+</sup> ion concentration in the cell, which causes the in-flow of Na<sup>+</sup> ions rather than the out-flow of the gel upon voltage.<sup>[32]</sup> The recovery in the structural color can be achieved by immersing the hydrogel in water for about 4 hours (**Figure S6**).

In addition to ions exchange, the migration of hydrated Na<sup>+</sup> and H<sup>+</sup> in the gel will also affect the swelling/deswelling of the gel. In the case of a perpendicular electric field, the migration of hydrated Na<sup>+</sup> ions (electrophoresis of hydrated Na<sup>+</sup>) in hydrogel is not predominant, because the diffusion of ions out of the gel into the surrounding water is easier than that in the gel. Additionally, the migration of hydrated ions through thousands of hydrophobic bilayer domains (with C24 long alkyl chains) may be inhibited compared to the diffusion of ions in and out of the hydrogel. Here the existence of the surrounding water near the hydrogel supplies the water source for the above reactions. We found that removing water around the hydrogel (with electrodes directly contacted to hydrogel) could also cause a blue shift of the structural color in a faster way. However, the hydrogel exhibited a significant anisotropic swelling with a shape bending to the anode (**Figure S7**).

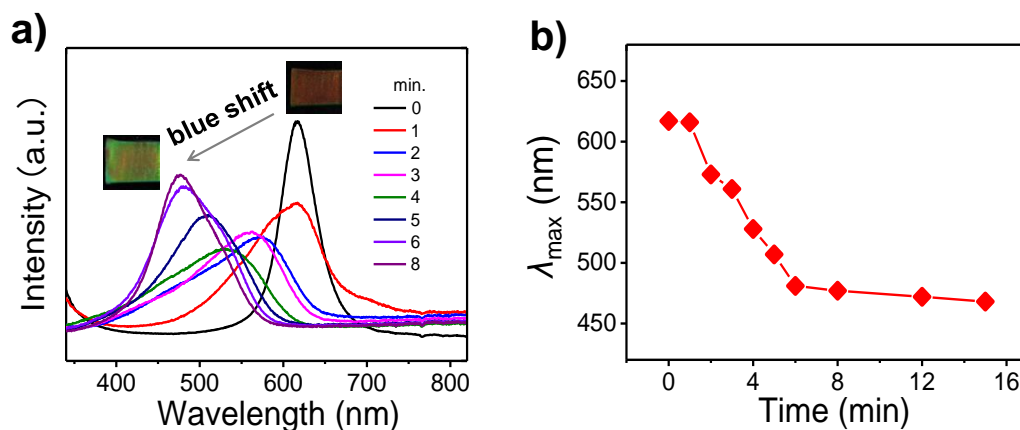


**Figure 3 Electro-optic responses in layered photonic hydrogels with electric field perpendicular to layers** a) The reflection wavelength change of the photonic hydrogel under electric field with time. b) The maximum wavelength ( $\lambda_{\max}$ ) decreases with increasing time at a voltage of 8.0 V.

### 2.3 Effect of parallel electric field

By applying an electric field parallel to the layers, the hydrogel is expected to change color from red to rainbow-like colors (**Figure 2d-e**). In this case, the water-swollen gel is set to be interposed between a pair of electrodes and the voltage is directly applied on the two edges of the gel (**Figure 2d**). Besides the effect of ions exchange, another main reason for the electric-optic response is the migration of charged ions ( $\text{Na}^+$  and  $\text{H}^+$ ) along layers towards the electrode bearing a charge opposite in sign to that borne by the polymer network (**Figure 2f**).<sup>[33]</sup> Additionally, the hydrated  $\text{Na}^+$  ions can migrate to the cathode side with water, resulting in the swelling of the hydrogel near the cathode-side to reflect near-infrared light. Between the cathode and anode, there is a gradient change in the

polyelectrolyte layers to show various colors. Thus, the hydrogel may exhibit rainbow-like structural colors.

**Figure 4** shows effects of applying a voltage of 8.0 V parallel to the layers of a red hydrogel. After directly applying 8.0 V for 2 min, the color of the hydrogel shifted from red to a unique rainbow-like color (**Figure 4a**). The side connected to the anode electrode appeared blue, while the side connected to the cathode changed to a near-infrared color. Between the two edges, an intermediate region with various discontinuously tunable visible colors was observed. **Figure 4b** illustrates that the photonic hydrogel was able to display position-dependent continuous shifts in reflected light, and the photonic stop band is swept throughout the visible spectrum to the near-infrared region stepwisely (450–850 nm). The time-dependent reflection spectrum at a fixed position of the hydrogel was also measured (**Figure S8**). Firstly, the intensity of the reflection spectrum at 710 nm decreased, which is associated with an anisotropic shrink in the region close to the anode. Then, a new peak (567 nm) appeared in the short wavelength region with time, indicating there are structures with two different bilayer distances. Finally, the peak in the long wavelength region disappeared and the peak at the short wavelength region continuously increased its intensity (**Figure S8**). The large electro-optic response from the visible to the near-infrared region is attributed to the significant layer distance change under electric stimuli. The layer distance was tuned from 195 nm to 369 nm, as calculated from Bragg's diffraction equation,  $\lambda = 2nd\sin\theta$ , where  $n$  is the average refractive index of the high-water-content hydrogel ( $n=1.33$ ),  $d$  is the distance of the layer from the diffracting plane,

and  $\theta$  is the Bragg glancing angle. The large and dramatic color tunability resulted from the swelling/shrinking behavior of the layered hydrogel under an electric field parallel to the layers (**Figure S9**).

In the case of a parallel electric field, the same electrochemical reaction occurs near the electrode, i.e., the water contained in the hydrogel is rapidly electrolyzed into  $H^+$  ions on the anode side. In addition to the ions exchange from  $-COONa$  to  $-COOH$ , the large shrinkage of the hydrogel near the anode is also due to the loss of water because there is no surrounding water (**Figure 2d**). Some of the water moves to the cathode with mobile ions, and some of water is consumed by the electrochemical reaction (~22 wt% of water was consumed by the reaction after applied 8.0 V for 2 min) (**Figure S9**). Without surrounding water, the hydrated ions ( $Na^+$  and  $H^+$ ) move to the cathode along the gel layers, swelling that region (cathode) of the hydrogel to reflect near-infrared light. The ion migration is governed by both the number of mobile ions and the electric field. Here the hydrated ions migration along the layers are easier than that perpendicular to the layers because the bilayer domains are hydrophobic. At the same time, the electrostatic attraction of negatively charged carboxyl groups toward the anode side creates a uniaxial stress along the layer axis, which leads to the deformation of the hydrogel from an oblong shape to a V-shape.<sup>[24]</sup>

The prominent swelling/shrinking behavior of the hydrogel can be identified from the thickness change of the cross section along the layer axis (**Figure 4c**). The cross-section view of the hydrogel showed a ladder-stepping shape with increasing thickness. The

discontinuously color change is due to the stepwise swelling behavior which is probably due to the different hydrated ions migration from anode to cathode. The  $\text{Na}^+$  ions immediately migrate to the cathode once upon applying parallel electric field, while the  $\text{H}^+$  ions gradually appear after water electrolysis and migrate to the cathode with a delayed time. **Figure 4d** illustrates the varying thickness and layer distance along the layer axis ( $X/W$ ), where  $X$  is the distance from the anode, and  $W$  is the total distance from anode to cathode. **Figure 4d** also shows the ladder-stepping change where the thickness values of the near-infrared (cathode) and blue regions (anode) were approximately 1.6 mm and 0.75 mm, respectively.

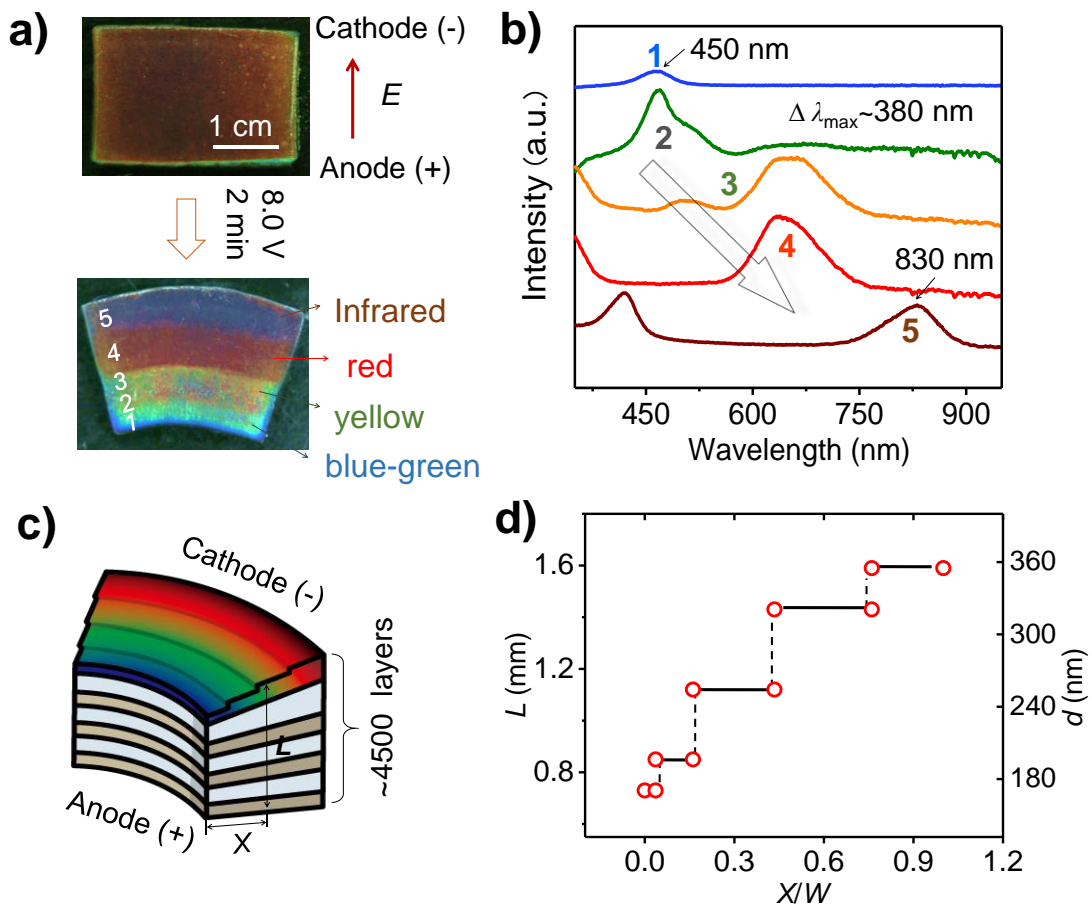




**Figure 4 Electro-optic responses in layered photonic hydrogels with electric field parallel to layers.** a) After applying 8.0 V to the cell, the color of the hydrogel shifts from homogeneous red to rainbow-like color. b) The reflection spectra in different positions of the rainbow-like hydrogel surface, as labelled 1-5 in a). c) Schematic diagram of the rainbow-like photonic gel and the layer structure with cross-section showing varying thickness. d) Hydrogel thickness ( $T$ ) and layer distance ( $d$ ) shows a step-like increase along the layer in the direction from the side connected with anode to the side close to cathode ( $X$  is the distance from the anode, and  $W$  is the total sample width).

#### **2.4 Electric patterning on photonic hydrogels**

To the best of our knowledge, most of the studies on electrically tunable photonic crystals or hydrogels report structural color changes without the formation of patterns. So far, electrically controlled display systems have been primarily limited to liquid system or ink of colloidal crystals, where the periodic structure is stable in the system by physical interaction. Attain fast and reversible electric display patterns in a solid-state system is still challenging because it is difficult to selectively change the periodic structure that is covalently fixed in the polymer network.

Due to the fractured bilayer structures embedded in ultrahigh-water content (~98%) polyelectrolyte polymers, the layered hydrogel developed in this work displayed patterns by a simple method based on patterned electrodes that apply an electric field perpendicular to the layers for several seconds (**Figure 5**). For example, some characters

were drawn on an aluminum film with a knife by hand, and then placed the aluminum film on the surface of the photonic hydrogel. After applying an electric field (8.4 V) for 10 s, the drawing characters appeared on the photonic hydrogel with blue color (**Figure 5a-b, Figure S10**). The regions that directly contacted the anode electrode quickly changed color from red to blue within 10 s. Other designed characters/patterns were also appeared on the photonic hydrogel by repeatedly electrically patterning and erasing patterns in water (**Figure 5c**). This electric patterning is very fast in a few seconds, which is mainly due to the loss of water on the regions that contacted with the anode. The electrolysis of water and the migration of hydrated  $\text{Na}^+$  ions, resulting in the loss of water on the patterned regions immediately. The loss of water reduced the layer distance and thus a blue shift in the structural colors (**Figure S11**). After removing the electric field, these patterns still remained on the hydrogel for ~1-2 h in water without consuming any energy (**Movie 2**), indicating its energy-saving display ability, whereas other electric devices are generally energy-consuming and display weakly underwater. When the cations in the water gradually enter the polymer network, the patterns disappear, the photonic hydrogel recovers to the initial far-red color, and it was ready for the next electric patterning for rewritable purposes. The pattern disappearing speed was affected by the ion concentrations (e.g.,  $\text{Na}^+$ ) in the exterior solution. When the exterior solution (water) was very pure with almost no cations, the hydrogel maintained the patterns for a longer time underwater. A slight increase in the  $\text{Na}^+$  concentration in the solution resulted in a faster disappearance of the patterns due to the rapid ion migration from the exterior

solution into the polymer network.

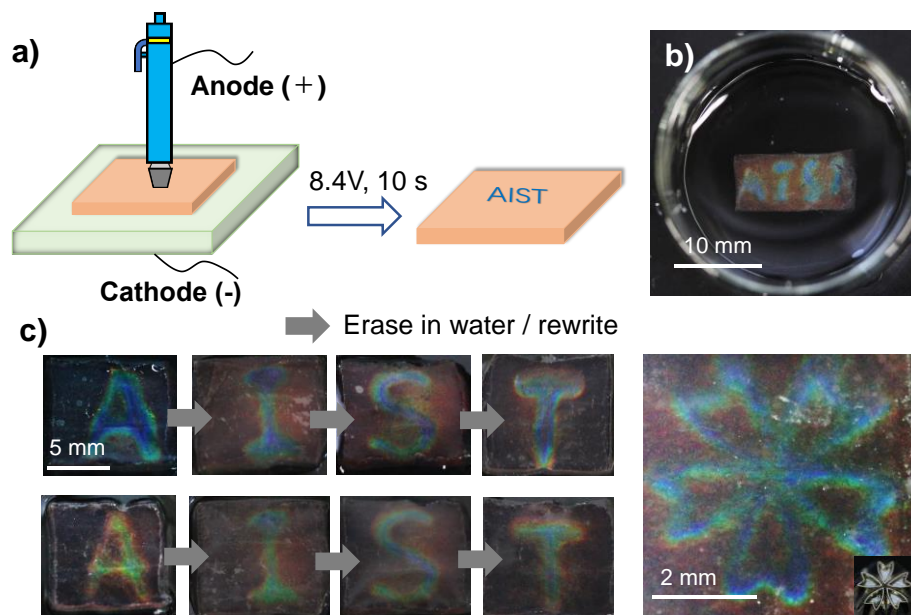


**Figure 5 Electric patterning on the layered photonic hydrogel.** (a) Schematic illustration of electrically patterning on the hydrogels by using a patterned electrode as anode and a bottom un-patterned electrode as cathode. The hydrogel was directly in contact to the two electrodes. (b) After removing the electrodes, the layered hydrogel displays the designed patterns in water. (c) Different patterns are applied continuously on the same place of the same sample. The structural color of patterns in the bottom row changes after immersing in water for several minutes.

### 2.5 Resolution, response time, and reversibility

Resolution, response time, and reversibility are important parameters for electrically tunable photonic hydrogels. An aluminum film with a thickness of  $\sim 40 \mu\text{m}$  was used as sample to check the resolution limits of the photonic hydrogels under electric patterning. The thin side of the aluminum film was placed onto one side of the hydrogel and used as

the anode. Once under an electric field (8.4 V) for only 3 s, the strip lines were clearly printed on the photonic hydrogel (**Figure 6**). The size of the electrode was limited by the minimum thickness of the aluminum film. However, it can create arrays of lines within a size of 30  $\mu\text{m}$  (**Figure 6a**). In particular, such printing on the photonic hydrogel was achieved with a low electric voltage (8.4 V) for a short time (3 s), indicating that this layered photonic hydrogel is among the fastest and most electrically responsive photonic crystals reported so far. Within such a short time, a thickness difference of  $\sim 50 \mu\text{m}$  was achieved compared with the regions without an electric field (**Figure 6a-b**). Such electrically induced surface patterning not only modulate the structural color, but also supply an effective strategy for producing spatial micropatterned surface which is confirmed to be important for aligning cells and manipulating cell functions on the hydrogel.<sup>[34]</sup> Additionally, the cyclic reversibility (electrically patterning/erasing) of the photonic hydrogels under an electric field was found to be good (**Figure 5c**). The electric-produced pattern on the hydrogel can be erased automatically in water for several hours. Then a new pattern can be rewritten by a new patterned electrode on the same position of the sample. More than ten electrical patterning cycles were performed on the same sample without any obvious color decay.

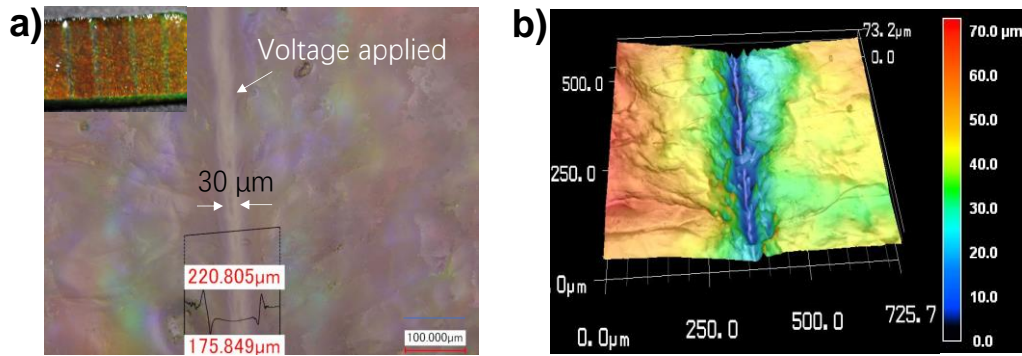


**Figure 6 Electrically induced microscale patterning on photonic hydrogels.** a) The optical microscopic image of the photonic hydrogel patterned with a line upon electric field (perpendicular to the layers). The macroscopic photo was inserted in the top left. b) Surface three-dimensional height maps of the electrically patterned regions using laser scanning confocal microscopy.

### 3. Conclusions

In this work, we demonstrated that an ultrahigh-water-content 1D photonic hydrogel showed large electro-optic responses in all visible to near-infrared wavelength region. The layered photonic hydrogel exhibited different color tunability under perpendicular or parallel electric fields in the directions of the hydrogel layers. It exhibited uniform color tuning when a perpendicular electric field was applied, while it showed a unique rainbow-like color from blue to near-infrared when applying a parallel electric field to the layers. Additionally, the hydrogel maintained the electrically printed patterns for a long time underwater. Such electrical optical modulation, in full-color to near infrared wavelength, gives complementary choices for the design of next-generation reflective displays for under water applications. Issues such as angle-dependent visualization and switching

rates still need to be resolved for the production of displays based on this technology. However, it is believed that the thin-film form, low drive voltages, flexibility, reversibility, and high reflectivity of the layered photonic hydrogel offer a convenient, economical, and eco-friendly method to develop displays for underwater applications (*e.g.*, in an aquarium) because traditional electrical devices are generally energy-consuming and display weakly underwater.

#### **4. Experimental section**

*Synthesis of electrically tunable ultrahigh-water-content photonic hydrogels.*

Ultrahigh-water-content photonic hydrogels were synthesized by chemical treatment of the parent photonic hydrogels. The parent photonic hydrogels were synthesized according to a previous study as follows <sup>[26]</sup>: an aqueous solution of 0.10 M DGI, 0.027 mol% sodium dodecyl sulfate relative to DGI, 2M AAm, 2.5 mM N, N'-methylenebis acrylamide (cross-linker), and 2 mM Irgacure 2959 (initiator) was mixed in a glass bottle at room temperature (25 °C). The solution was kept in a water bath (55 °C) for 4 h to reach the equilibrium state. Then, the solution was injected into a glass cell (0.5mm spacing) applying shear flow using a pipette. The shear flow induced bilayer orientation parallel to the glass substrates. Then, radical polymerization was performed by UV light at 50 °C for ~8 h. After polymerization, the gel was immersed in water for 1 week to reach an equilibrium swelling state. The parent photonic hydrogels had a water content of ~90wt% and they showed no response to the electric field. To produce an electrically tunable photonic

hydrogel, the parent photonic hydrogel was treated in 1 M NaOH aqueous solution (10ml) for 40 s at 57 °C. Before the NaOH treatment, the gel was immersed in 1 M NaOH at room temperature to achieve a homogenous state. The obtained polyelectrolyte hydrogel swells in water largely due to the chemical group change from  $-\text{CONH}_2$  into carboxylate group ( $-\text{COONa}$ ). The water content of the prepared polyelectrolyte photonic hydrogels was measured to be 97.7wt%. The NaOH treatment time affects the swelling degrees and  $-\text{COONa}$  contents in the polymer networks.<sup>[28]</sup> The hydrogel with shorter treatment time shows a smaller wavelength shift (**Figure S12**). In general, the common hydrogels (such as PAAcNa gel) are usually brittle under conditions of ultrahigh-water-content that above 97 wt%, and thus have small recoverable deformation due to their high water content and fragile network in a fully swollen state.<sup>[35]</sup> However, these prepared high-water-content photonic hydrogels can still be mechanically deformed to a large extent (strain: 80%) and remain stable under electrical stimulation, which is mainly due to the existence of nanoscale bilayer domains that toughened the materials.

#### *Electric patterning on the photonic hydrogels.*

Typically, a pattern was carved in a thin metal (e.g., aluminum) sheet with a knife. The patterned metal sheet was placed on the photonic hydrogels as an anode, and another metal electrode (without patterning) was placed below the photonic hydrogel as a cathode. Both electrodes were directly contacted to the hydrogel. After applying an electric field (8.4 V) for several seconds, the designed pattern appeared on the photonic hydrogels. The patterns on the photonic hydrogels were stable for about 1-2 h when the hydrogel was

immersed in water. Other patterns or micropatterns can also be printed on the photonic hydrogels using the same methods.

## References

- [1] P. Vukusic, J. R. Sambles, *Nature* **2003**, *424*, 852.
- [2] E. Yablonovitch, *Phys. Rev. Lett.* **1987**, *58*, 2059.
- [3] J. D. Joannopoulos, P. R. Villeneuve, S. Fan, *Nature* **1997**, *386*, 143.
- [4] J. Ge, Y. Yin, *Angew. Chemie Int. Ed.* **2011**, *50*, 1492.
- [5] X.-Y. Lei, H. Li, F. Ding, W. Zhang, N.-B. Ming, *Appl. Phys. Lett.* **1997**, *71*, 2889.
- [6] C. Fenzl, T. Hirsch, O. S. Wolfbeis, *Angew. Chemie Int. Ed.* **2014**, *53*, 3318.
- [7] A. K. Yetisen, H. Butt, F. da Cruz Vasconcellos, Y. Montelongo, C. A. Davidson, J. Blyth, L. Chan, J. B. Carmody, S. Vignolini, U. Steiner, J. J. Baumberg, T. D. Wilkinson, C. R. Lowe, *Adv. Opt. Mater.* **2014**, *2*, 250.
- [8] Y. Yue, X. Li, T. Kurokawa, M. A. Haque, J. P. Gong, *J. Mater. Chem. B* **2016**, *4*, 4104.
- [9] Y. Yue, T. Kurokawa, *ACS Appl. Mater. Interfaces* **2019**, *11*, 10841.
- [10] M. Malekovic, M. Urann, U. Steiner, B. D. Wilts, M. Kolle, *Adv. Opt. Mater.* **2020**, *8*, 2000165.
- [11] Y. Yue, J. P. Gong, *J. Photochem. Photobiol. C Photochem. Rev.* **2015**, *23*, 45.
- [12] K. Ueno, K. Matsubara, M. Watanabe, Y. Takeoka, *Adv. Mater.* **2007**, *19*, 2807.



- [13] A. C. Arsenault, D. P. Puzzo, I. Manners, G. A. Ozin, *Nat. Photonics* **2007**, *1*, 468.
- [14] J. J. Walish, Y. Kang, R. A. Mickiewicz, E. L. Thomas, *Adv. Mater.* **2009**, *21*, 3078.
- [15] I. Lee, D. Kim, J. Kal, H. Baek, D. Kwak, D. Go, E. Kim, C. Kang, J. Chung, Y. Jang, Others, *Adv. Mater.* **2010**, *22*, 4973.
- [16] L. Liu, S. K. Karuturi, L. T. Su, Q. Wang, A. I. Y. Tok, *Electrochem. commun.* **2011**, *13*, 1163.
- [17] K. Chen, Q. Fu, S. Ye, J. Ge, *Adv. Funct. Mater.* **2017**, *27*, 1702825.
- [18] W. Wang, X. Fan, F. Li, J. Qiu, M. M. Umair, W. Ren, B. Ju, S. Zhang, B. Tang, *Adv. Opt. Mater.* **2018**, *6*, 1701093.
- [19] Y. Xie, Y. Meng, W. Wang, E. Zhang, J. Leng, Q. Pei, *Adv. Funct. Mater.* **2018**, *28*, 1802430.
- [20] Q. Fu, H. Zhu, J. Ge, *Adv. Funct. Mater.* **2018**, *28*, 1804628.
- [21] H.-K. Chang, J. Park, *Adv. Opt. Mater.* **2018**, *6*, 1800792.
- [22] D. Y. Kim, S. Choi, H. Cho, J.-Y. Sun, *Adv. Mater.* **2019**, *31*, 1804080.
- [23] T. Tanaka, I. Nishio, S.-T. Sun, S. Ueno-Nishio, *Science*. **1982**, *218*, 467.
- [24] J. Gong, T. Nitta, Y. Osada, *J. Phys. Chem.* **1994**, *98*, 9583.
- [25] T. Tsujii, Kaoru and Hayakawa, Masaki and Onda, Tomohiro and Tanaka, *Macromolecules* **1997**, *30*, 7397.
- [26] M. A. Haque, G. Kamita, T. Kurokawa, K. Tsujii, J. P. Gong, *Adv. Mater.* **2010**,

- 22, 5110.
- [27] Y. F. Yue, M. A. Haque, T. Kurokawa, T. Nakajima, J. P. Gong, *Adv. Mater.* **2013**, *25*, 3106.
- [28] Y. Yue, T. Kurokawa, M. A. Haque, T. Nakajima, T. Nonoyama, X. Li, I. Kajiwara, J. P. Gong, *Nat. Commun.* **2014**, *5*, 4659.
- [29] M. A. Haque, T. Kurokawa, G. Kamita, J. P. Gong, *Macromolecules* **2011**, *44*, 8916.
- [30] X. Li, T. Kurokawa, R. Takahashi, M. A. Haque, Y. Yue, T. Nakajima, J. P. Gong, *Macromolecules* **2015**, *48*, 2077.
- [31] S. Sakohara, F. Muramoto, M. Asaeda, *J. Chem. Eng. Japan* **1990**, *23*, 119.
- [32] S.-B. Lin, C.-H. Yuan, A.-R. Ke, Y.-L. Li, N. Ouyang, *Adv. Polym. Technol.* **2013**, *32*, 20.
- [33] R. Kishi, Y. Osada, *J. Chem. Soc. Faraday Trans. 1 Phys. Chem. Condens. Phases* **1989**, *85*, 655.
- [34] J. Leijten, J. Seo, K. Yue, G. Trujillo-de Santiago, A. Tamayol, G. U. Ruiz-Esparza, S. R. Shin, R. Sharifi, I. Noshadi, M. M. Álvarez, Y. S. Zhang, A. Khademhosseini, *Mater. Sci. Eng. R Reports* **2017**, *119*, 1.
- [35] Y. Si, L. Wang, X. Wang, N. Tang, J. Yu, B. Ding, *Adv. Mater.* **2017**, *29*, 1700339.